



# Recovery from tachyphylaxis of TRPV1 coincides with recycling to the surface membrane

Quan Tian<sup>a,1</sup>, Juan Hu<sup>a,1</sup>, Chang Xie<sup>a,1</sup>, Kaidi Mei<sup>a</sup>, Cuong Pham<sup>b</sup>, Xiaoyi Mo<sup>a</sup>, Régine Hepp<sup>b</sup>, Sylvia Soares<sup>b</sup>, Fatiha Nothias<sup>b</sup>, Yuanyuan Wang<sup>a</sup>, Qiang Liu<sup>a</sup>, Fen Cai<sup>a</sup>, Bo Zhong<sup>a</sup>, Dongdong Li<sup>b,2</sup>, and Jing Yao<sup>a,2</sup>

<sup>a</sup>Hubei Key Laboratory of Cell Homeostasis, College of Life Sciences, Wuhan University, Wuhan, 430072 Hubei, China; and <sup>b</sup>Sorbonne Université, Institut de Biologie de Paris-Seine, Neuroscience Paris Seine, CNRS UMR8246, INSERM U1130, 75005 Paris, France

Edited by Francisco Bezanilla, The University of Chicago, Chicago, IL, and approved January 31, 2019 (received for review November 20, 2018)

**The transient receptor potential vanilloid-1 (TRPV1) ion channel is essential for sensation of thermal and chemical pain. TRPV1 activation is accompanied by Ca<sup>2+</sup>-dependent desensitization; acute desensitization reflects rapid reduction in channel activity during stimulation, whereas tachyphylaxis denotes the diminution in TRPV1 responses to repetitive stimulation. Acute desensitization has been attributed to conformational changes of the TRPV1 channel; however, the mechanisms underlying the establishment of tachyphylaxis remain to be defined. Here, we report that the degree of whole-cell TRPV1 tachyphylaxis is regulated by the strength of inducing stimulation. Using light-sheet microscopy and pH-sensitive sensor pHluorin to follow TRPV1 endocytosis and exocytosis trafficking, we provide real-time information that tachyphylaxis of different degrees concurs with TRPV1 recycling to the plasma membrane in a proportional manner. This process controls TRPV1 surface expression level thereby the whole-cell nociceptive response. We further show that activity-gated TRPV1 trafficking associates with intracellular Ca<sup>2+</sup> signals of distinct kinetics, and recruits recycling routes mediated by synaptotagmin 1 and 7, respectively. These results suggest that activity-dependent TRPV1 recycling contributes to the establishment of tachyphylaxis.**

desensitization | calcium | synaptotagmin | pain | TRP channel

**T**ransient receptor potential vanilloid-1 (TRPV1) is a Ca<sup>2+</sup>-permeable cation channel expressed in sensory nerves specialized for pain detection (1, 2). Ca<sup>2+</sup> influx upon TRPV1 activation induces channel desensitization, with acute desensitization referring to the rapid reduction in the evoked inward current, and tachyphylaxis denoting current diminutions over repetitive stimulation (1, 3, 4). Desensitization can be leveraged to treat clinical pain. For instance, the TRPV1 agonist capsaicin has been used as a therapeutic analgesic (5, 6).

The mechanism underlying TRPV1 acute desensitization has been widely explored and converged on agonist-induced conformational changes at the channel level (1, 2). In this regard, TRPV1 interacts in a Ca<sup>2+</sup>-dependent manner with either or both calcineurin (7), calmodulin (8), and phosphatidylinositol 4,5-bisphosphate (9), to regulate channel gating and inactivate response. Relatively, much remains to be understood on the mechanisms underlying the establishment of tachyphylaxis. Early studies show that phosphorylation of TRPV1 by protein kinase A and mutation at the corresponding phosphorylation site affect the induction of tachyphylaxis, which yet display little effect on acute desensitization (1, 7, 10). Likely, the establishment of tachyphylaxis recruits other mechanisms besides those assigned for acute desensitization.

Here, we observed by whole-cell patch clamp that the extent of tachyphylaxis is regulated by the strength of inducing stimulation. Imaging TRPV1 exocytosis and endocytosis trafficking in real time by light-sheet microscopy and a pH-sensitive sensor, we show that TRPV1 channels undergo activity-dependent recycling to control their surface expression thereby the strength of whole-cell desensitization. We also show that stimulation of different strengths elicits intracellular Ca<sup>2+</sup> signals of different kinetics

and regulates TRPV1 recycling via distinct routes mediated by synaptotagmin 1 and 7, respectively. These results suggest the contribution of TRPV1 trafficking to the establishment of tachyphylaxis.

## Results

**Whole-Cell Tachyphylaxis Is Stimulation Strength Dependent.** TRPV1 tachyphylaxis is a Ca<sup>2+</sup>-dependent process and has been induced by saturated doses of capsaicin (1, 4, 9). We applied different doses of capsaicin to induce desensitization in TRPV1-expressing HEK 293 cells. A reference current was evoked by 1 μM capsaicin in the absence of Ca<sup>2+</sup> at the beginning. Then in the presence of external Ca<sup>2+</sup> (Fig. 1 *A–D*, color bar), capsaicin stimulation led whole-cell responses to a tachyphylaxis state. Subsequent stimulation by similar doses only elicited a much reduced response (Fig. 1 *A–D*). Tachyphylaxis is known to reduce the agonist affinity of TRPV1, rather than its loss of function (1). Indeed, following low (0.3 or 1 μM) capsaicin-induced tachyphylaxis, increasing subsequent stimulation to supramaximal range (5–100 μM capsaicin) evoked whole-cell currents approaching the pretachyphylaxis level (Fig. 1 *A, B*, and *E*, blue and green vs. black).

However, as for the tachyphylaxis induced by relatively high doses of capsaicin (3–10 μM), the supramaximal stimulations

## Significance

**TRPV1 ion channel plays an important role in the transmission and modulation of pain. Desensitization of TRPV1 in nociceptors is adaptable for analgesic therapy. One type of desensitization is tachyphylaxis that reflects reduced TRPV1 responses to repetitive stimuli. To understand the mechanism underlying the whole-cell tachyphylaxis, here we used an orthogonal electro-optical approach integrating electrophysiology and light-sheet microscopy. We show that the intensity of tachyphylaxis is regulated by the strength of inducing stimulation, and that TRPV1 channels undergo activity-gated recycling to regulate their surface expression level thereby the degree of tachyphylaxis. This study provides real-time insights into the establishment of tachyphylaxis and helps to understand desensitization-based analgesics.**

Author contributions: D.L. and J.Y. designed research; Q.T., J.H., C.X., K.M., C.P., X.M., Y.W., Q.L., F.C., D.L., and J.Y. performed research; R.H., S.S., F.N., and B.Z. contributed new reagents/analytic tools; Q.T., J.H., C.X., K.M., X.M., Y.W., Q.L., F.C., D.L., and J.Y. analyzed data; and D.L. and J.Y. wrote the paper.

The authors declare no conflict of interest.

This article is a PNAS Direct Submission.

Published under the PNAS license.

<sup>1</sup>Q.T., J.H., and C.X. contributed equally to this work.

<sup>2</sup>To whom correspondence may be addressed. Email: dongdong.li@inserm.fr or jyao@whu.edu.cn.

This article contains supporting information online at [www.pnas.org/lookup/suppl/doi:10.1073/pnas.1819635116/-DCSupplemental](http://www.pnas.org/lookup/suppl/doi:10.1073/pnas.1819635116/-DCSupplemental).

Published online February 25, 2019.

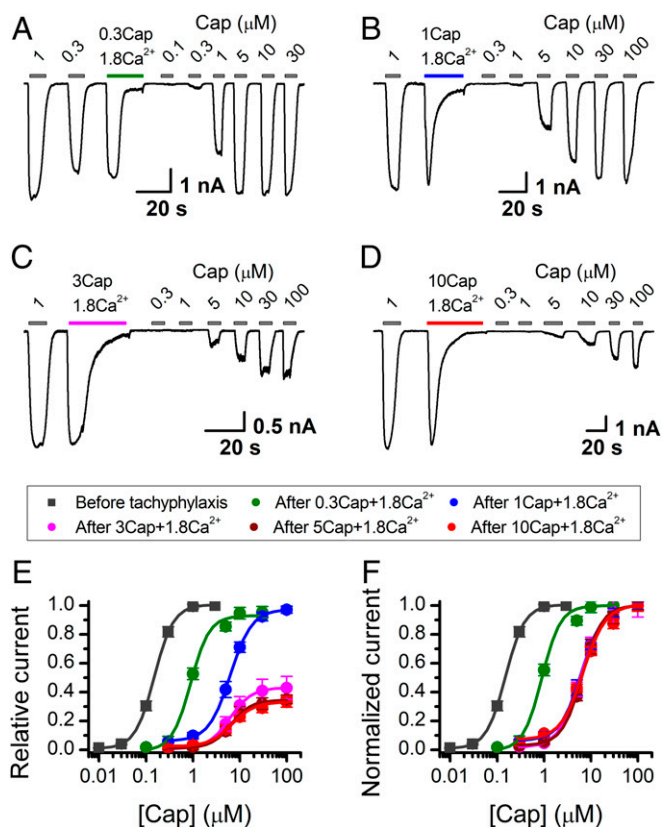


**Fig. 1.** Tachyphylaxis is regulated by the strength of preimposed stimulation. (A–D) Representative traces showing repetitive activation of TRPV1 channels after desensitization induced by 0.3  $\mu\text{M}$ , 1  $\mu\text{M}$ , 3  $\mu\text{M}$ , and 10  $\mu\text{M}$  capsaicin in the presence of  $\text{Ca}^{2+}$  (1.8 mM), as indicated by the color bars. Responses shown under gray bars were recorded in the absence of external  $\text{Ca}^{2+}$  to prevent further desensitization and gain whole-cell responses. A small current appeared upon the washing out of  $\text{Ca}^{2+}$ , reflecting its inhibitory effect on TRPV1 activity as reported (42). The pipette solution contained no adenosine triphosphate (ATP). (E) Dose–response curves for whole-cell TRPV1 currents obtained before and after tachyphylaxis induction. Data are shown as relative values to the reference current evoked by 1  $\mu\text{M}$  capsaicin at the beginning of each recording. Solid lines are fits to Hill equation ( $n = 7\text{--}18$  cells for each condition). (F) Dose–response curves normalized to their intrinsic maximum. Recordings were from transiently transfected HEK 293 cells held at  $-60$  mV. Cap, capsaicin. Error bars, SEM.

could not trigger currents close to the pretachyphylaxis level (Fig. 1C and D). The derived dose–response curves ended at a much lower level than that observed for low capsaicin-induced tachyphylaxis (Fig. 1E). Hence, the degree of tachyphylaxis, namely the inhibitory effect on whole-cell TRPV1 current, is dependent on the strength of the inducing stimulation.

Notably, though 1  $\mu\text{M}$  and 3–10  $\mu\text{M}$  capsaicin all lie in the saturation range in evoking TRPV1 whole-cell current under control condition (Fig. 1E, gray square), they induced tachyphylaxis to different extents (Fig. 1E, blue vs. reddish). Apart from the subsaturation dose (Fig. 1F, green), all saturated doses of capsaicin (1–10  $\mu\text{M}$ ) caused an almost identical right-shift in normalized dose–response curves (Fig. 1F, blue and reddish), indicating a similar reduction in the agonist affinity of TRPV1. Thus, tachyphylaxis of varied degrees induced by distinct saturated doses of capsaicin, could not be explained by the reduction in TRPV1 agonist affinity and would have recruited other mechanistic pathways.

**Light-Sheet Imaging of TRPV1 Trafficking.** TRPV1 expression level at the plasma membrane is another factor in shaping whole-cell

nociceptive responses (11, 12) and has been suggested to be regulated by TRPV1 exocytosis and endocytosis (13, 14). To explore TRPV1 trafficking in real time, we engineered a TRPV1 fusion protein comprising the pH-dependent green fluorescent protein (GFP) mutant pHluorin that is green fluorescent in a neutral condition and dim in an acidic environment (15). The electrophysiological property of TRPV1 was unaffected by the insertion of pHluorin (SI Appendix, Fig. S1). In our configuration, TRPV1-pHluorin is dim when trapped into acidic trafficking vesicles and of high fluorescence upon exocytic insertion into the plasma membrane (SI Appendix, Fig. S2A). We could then follow TRPV1 surface expression and subcellular trafficking by dynamic imaging of pHluorin fluorescence.

To gain high-quality imaging, and avoid potential phototoxicity of laser scanning microscopy, we have used light-sheet microscopy that enables scanless optical sectioning and wide-field image acquisition by digital camera (16). Light sheet of  $\mu\text{m}$ -scale thickness and perpendicular to the optical axis of imaging objective, was generated via an orthogonally placed excitation objective (SI Appendix, Fig. S2B). The thin light sheet evidently improved the image quality of TRPV1-pHluorin-expressing HEK cells relative to conventional epifluorescence (SI Appendix, Fig. S2B, Right). A supramaximal dose of capsaicin caused a pronounced diminution in TRPV1-pHluorin fluorescence followed by a gradual recovery (SI Appendix, Fig. S2C), reflecting the retrieval of TRPV1 channels by endocytosis and their reinsertion by subsequent exocytosis. Inhibiting general endocytosis pathways by hypertonic solution (17) largely blocked the capsaicin-evoked fluorescence diminution (SI Appendix, Fig. S2D and F), with a transient increase unmasked that implies the co-occurrence of exocytosis. Further, omission of external  $\text{Ca}^{2+}$  inhibited both the exocytosis and endocytosis of TRPV1-pHluorin (SI Appendix, Fig. S2E and F), confirming the  $\text{Ca}^{2+}$ -dependence of TRPV1 recycling (1, 18, 19). Together, light-sheet imaging of TRPV1-pHluorin enables real-time mapping of TRPV1 trafficking and surface expression.

**Stimulation Strength Regulates TRPV1 Recycling.** To examine TRPV1 surface expression during strength-gated tachyphylaxis, we imaged TRPV1-pHluorin in HEK 293 cells upon 1 and 10  $\mu\text{M}$  capsaicin stimulation in the presence of external  $\text{Ca}^{2+}$ . While both stimuli evoked an initial loss in TRPV1 surface expression followed by a subsequent recovery, the high-dose capsaicin induced a significantly greater reduction in TRPV1 expression ( $-0.68 \pm 0.04$ , vs.  $-0.43 \pm 0.03$ ,  $P < 0.01$ ) followed by a much delayed recovery (Fig. 2A–C). At 5 min after 1  $\mu\text{M}$  capsaicin stimulation, TRPV1 surface expression recovered to about 95% of the control level, while with 10  $\mu\text{M}$  capsaicin stimulation, TRPV1 expression only recovered to 48% of the initial level at the same time point (Fig. 2D,  $P < 0.01$ ). Thus, stimulation of distinct strengths evoked TRPV1 recycling in a different manner and resulted in proportional loss in TRPV1 surface expression. The delayed recovery in TRPV1 surface expression level induced by high capsaicin renders the post-tachyphylaxis currents persistently inferior to those obtained after low capsaicin stimulation (Fig. 1E, red vs. blue).

The dependence of TRPV1 trafficking on stimulation strength was further confirmed by using varied doses of capsaicin (Fig. 2E). A small overshoot was noted in recovery phase of 1  $\mu\text{M}$  capsaicin stimulation (Fig. 2A), which in fact gradually went back to the initial level as revealed by a longer period of imaging (Fig. 2F, 20 min). The transient overshoot, therefore, reflects a transitory step for TRPV1 expression recovery. In contrast, the loss in TRPV1 expression caused by 10  $\mu\text{M}$  capsaicin persisted even over a long imaging period (Fig. 2F). Juxtaposing the time course of patch-clamp current and the TRPV1-pHluorin fluorescence validated the correlation between the loss in surface TRPV1 expression and the reduction in whole-cell response (SI Appendix, Fig. S3).

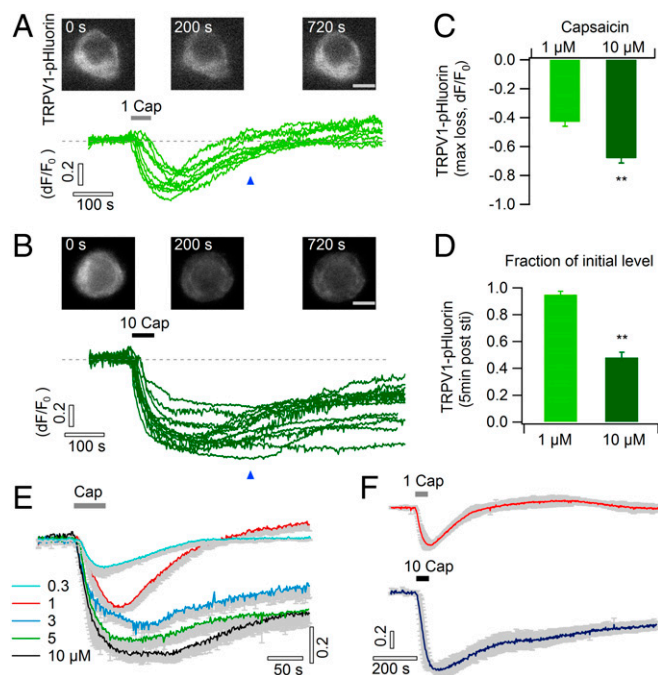


**Fig. 2.** TRPV1 channels undergo activity-dependent endocytosis and exocytosis recycling. (A) HEK cells expressing TRPV1-pHluorin and stimulated by 1  $\mu\text{M}$  capsaicin. Each single trace was derived from an individual cell, with a ring-shape region of interest (ROI) traced along the cell surface while excluding nucleus hole. Fluorescence change is expressed as  $dF/F_0$  with  $F_0$  as the mean intensity of prestimulation baseline. (B) HEK cells expressing TRPV1-pHluorin and stimulated by 10  $\mu\text{M}$  capsaicin. (C) The peak loss in TRPV1-pHluorin fluorescence for 1  $\mu\text{M}$  ( $n = 10$  cells) and 10  $\mu\text{M}$  capsaicin (13 cells) stimulation. (D) Recovery in TRPV1-pHluorin level quantified as the fraction to the prestimulation control level. The timing when the values were measured is indicated by blue arrowheads in A and B. (E) TRPV1-pHluorin recycling triggered by varied doses of capsaicin (0.3–10  $\mu\text{M}$ ,  $n = 7$ –13 cells for each condition). (F) Imaging of TRPV1-pHluorin trafficking for a long period (20 min;  $n = 10$  for 1  $\mu\text{M}$ , and 8 for 10  $\mu\text{M}$  capsaicin). (Scale bars, 10  $\mu\text{m}$ .)

Collectively, we show that TRPV1 recycling is stimulation strength dependent, which shapes the channel expression level and whole-cell tachyphylaxis.

In parallel, we confirmed this phenomenon in primary dorsal root ganglia (DRG) neurons that express endogenous TRPV1 channels. Similar to the above results, low-dose capsaicin (1  $\mu\text{M}$ ) induced tachyphylaxis with whole-cell currents fully recovered by supramaximal doses of capsaicin (*SI Appendix, Fig. S4A and C*), a process to counteract agonist affinity reduction that was facilitated by additive acidification ( $\text{H}^+$ ) (20). The same manipulation, however, failed to recover the whole-cell current following high capsaicin-induced tachyphylaxis (10  $\mu\text{M}$ , *SI Appendix, Fig. S4B and D*), echoing the additional contribution of the reduction in TRPV1 surface expression. As observed with light-sheet imaging, low capsaicin induced a transient reduction in TRPV1 expression that was followed by a quick recovery, whereas high capsaicin evoked a more pronounced and persistent loss in TRPV1 expression level (*SI Appendix, Fig. S4E and F*).

**TRPV1 Exocytosis Assists Whole-Cell Current Recovery.** During tachyphylaxis induction, capsaicin elicited endocytosis retrieval of surface TRPV1 followed by exocytosis-mediated recovery. This process is regulated by the stimulation strength as determined by both stimulation dose (Figs. 1 and 2) and duration (Fig. 3A and B). We further pondered that suspending recording for a brief period right after tachyphylaxis induction could

facilitate the exocytic reinsertion of TRPV1 and the whole-cell currents. As expected, a 5-min pause augmented the whole-cell response after 1  $\mu\text{M}$  capsaicin-induced desensitization, compared with the condition without interim pause (Fig. 3C and F, blue vs. open circle). This observation is consistent with the almost full recovery of TRPV1 surface expression at  $\sim 5$  min after stimulation of low capsaicin (1  $\mu\text{M}$ , Fig. 2D). A 5-min pause also enhanced the whole-cell current over high capsaicin-induced tachyphylaxis (Fig. 3D and F, red vs. open square). Mirroring the partial recovery in TRPV1 surface expression upon high capsaicin stimulation (10  $\mu\text{M}$ , Fig. 2D), the 5-min interim pause was still unable to rescue whole-cell response to pretachyphylaxis level (Fig. 3F, red vs. gray). As corroboration, adding another 5-min pause (10 min, in total) further increased whole-cell current following high capsaicin stimulation (Fig. 3E and F, orange vs. red). Together, these results consolidate that facilitating the recovery in TRPV1 surface expression helps to rescue the whole-cell nociceptive response.

**$\text{Ca}^{2+}$  Signals During TRPV1 Recycling.** As  $\text{Ca}^{2+}$  signal regulates TRPV1 desensitization (1, 4) and subcellular trafficking (21), we probed the  $\text{Ca}^{2+}$  kinetics over low and high capsaicin stimulation. Dual-color light-sheet imaging was performed in HEK cells expressing TRPV1-pHluorin and also loaded with a red-fluorescent  $\text{Ca}^{2+}$  indicator Rhod-2, AM (Fig. 4A). The absence of their cross-talk was ensured by using spectrally excluded excitation light and band-pass filters (*SI Appendix, Fig. S5A*), and also validated by imaging cells only harboring a single fluorophore (*SI Appendix, Fig. S5B*). We observed over TRPV1 recycling robust  $\text{Ca}^{2+}$  rises in response to both low and high capsaicin stimulation (Fig. 4B). Notably, though the peak amplitude was similar for both stimuli,  $\text{Ca}^{2+}$  rises evoked by high-dose capsaicin appeared longer-lasting and remained high at 5 min after stimulation (Fig. 4C), corresponding to sustained loss in TRPV1 surface expression (Fig. 4D). Hence, high-dose capsaicin triggers long-lasting  $\text{Ca}^{2+}$  signal along with delayed recovery of TRPV1 expression.

We also observed that reducing external  $\text{Ca}^{2+}$  concentration prevented the loss in TRPV1 surface expression in response to high capsaicin (Fig. 4E), suggesting the amount of  $\text{Ca}^{2+}$  influx influences channel recycling. To evaluate directly the amount of  $\text{Ca}^{2+}$  influx triggered by low- and high-dose capsaicin, we blocked the internal  $\text{Ca}^{2+}$  buffering process by inhibiting endoplasmic reticulum  $\text{Ca}^{2+}$  ATPase with thapsigargin (22). In this condition, high-dose capsaicin was found to evoke a higher amount of  $\text{Ca}^{2+}$  influx than low-dose capsaicin (Fig. 4F;  $dF/F_0 = 0.86 \pm 0.06$  for 10 Cap vs.  $0.69 \pm 0.05$  for 1 Cap,  $n = 8$  cells for each condition,  $P < 0.05$ ). The slow recovery in high capsaicin-induced  $\text{Ca}^{2+}$  signal could also be a reduction in the efflux of  $\text{Ca}^{2+}$  from the cell. We therefore examined the activity of  $\text{Na}^+/\text{Ca}^{2+}$  exchanger (NCX), a principal pathway for activity-gated  $\text{Ca}^{2+}$  export powered by  $\text{Na}^+$  gradient across the plasma membrane (23). Inhibiting NCX upon capsaicin stimulation would unmask its operating activity as reflected by the slowing down in  $\text{Ca}^{2+}$  recovery rate. Inactivating NCX by omitting external  $\text{Na}^+$  [replaced by *N*-methyl-D-glucamine<sup>+</sup> (NMDG<sup>+</sup>)] delayed  $\text{Ca}^{2+}$  recovery in response to both low and high capsaicin stimulation, yet in the latter condition the recovery phase was less affected (Fig. 4G; reduction in declining rate,  $0.008 \pm 0.002$   $dF/F_0/\text{min}$  for 10 Cap, vs.  $0.013 \pm 0.003$   $dF/F_0/\text{min}$  for 1 Cap vs.;  $n = 7$  cells for each condition,  $P < 0.05$ ). This observation suggests that the operating activity of NCX is compromised upon high capsaicin challenge, which together with the greater amount of  $\text{Ca}^{2+}$  influx, contributes to the delayed recovery in evoked  $\text{Ca}^{2+}$  signals.

**Synaptotagmin Regulation of TRPV1 Recycling.** To understand the mechanism underlying  $\text{Ca}^{2+}$ -regulated TRPV1 recycling over tachyphylaxis induction, we studied the role of synaptotagmin

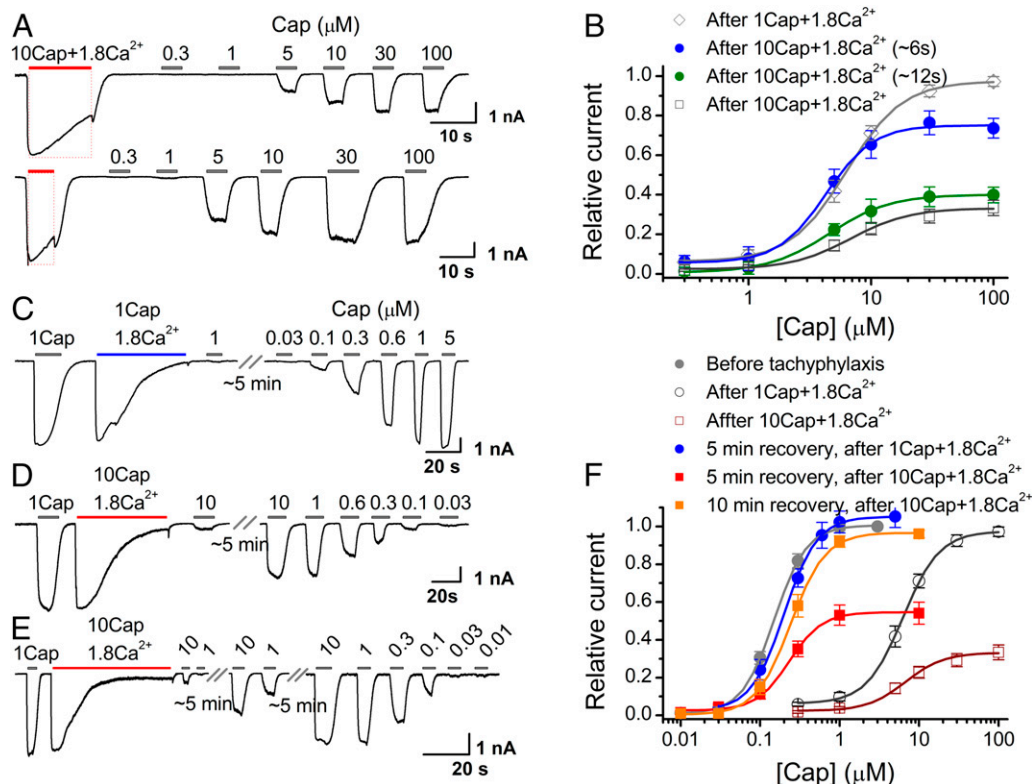


**Fig. 3.** Interim pause facilitates the restoration of whole-cell TRPV1 currents. (A) Whole-cell recording of a TRPV1-expressing HEK 293 cell. Desensitization was induced by 10  $\mu\text{M}$  capsaicin (1.8 mM  $\text{Ca}^{2+}$ ) over shorter periods (12 s, *Top*; 6 s, *Bottom*). (B) Dose–response curves of whole-cell currents during tachyphylaxis period. Data from briefer stimulation are compared with those obtained after normal stimulation durations ( $\sim 60$  s, gray traces). (C) After tachyphylaxis induced by 1  $\mu\text{M}$  capsaicin, current was hardly triggered by similar stimulation. A 5-min pause helped the recovery of whole-cell current to the pretachyphylaxis level. (D) Facilitating effect of interim pause seen for 10  $\mu\text{M}$  capsaicin-evoked desensitization. The facilitation was further enhanced by a longer pause period (5 min + 5 min; *E*). (F) Dose–response curves of whole-cell TRPV1 currents of different conditions, normalized to their initial reference current. Solid lines are fits to the Hill equation ( $n = 6$ –10 cells for each condition). The pipette solution contained 3 mM  $\text{Na}_2\text{ATP}$  and 3 mM  $\text{Mg}$  ATP. Error bars, SEM.

(Syt) proteins that serve as  $\text{Ca}^{2+}$  sensors in subcellular trafficking (24). Syt1 and Syt9 have been shown to interact with TRPV1 at the protein level by coimmunoprecipitation (co-IP) (18). We confirmed this result (Fig. 5A), and further found that Syt9 showed little effect on whole-cell TRPV1 responses during tachyphylaxis (*SI Appendix, Fig. S6 A and B*). Expression of Syt1 together with TRPV1 in HEK cells, albeit still leaving unchanged tachyphylaxis responses induced by high capsaicin (10  $\mu\text{M}$ ), facilitated the current recovery for low capsaicin-induced tachyphylaxis (1  $\mu\text{M}$ , Fig. 5 B and C, *light blue* vs. *gray circle*). This effect was prevented when mutating Syt1 to inactivate its  $\text{Ca}^{2+}$ -binding site [Syt1(4D/N)] (25) (Fig. 5C). Moreover, light-sheet imaging revealed a facilitating effect of Syt1 on TRPV1 expression recovery following 1  $\mu\text{M}$ , but not 10  $\mu\text{M}$  capsaicin stimulation (Fig. 5 D and H). These results suggest that Syt1 regulates fast TRPV1 recycling as triggered by low-dose capsaicin, while playing a marginal role in the slow recycling process following high capsaicin stimulation. This resembles the established role of Syt1 in regulating fast exocytosis near the plasma membrane (24). We also noted that Syt1 was preferentially expressed on cell surface (*SI Appendix, Fig. S7*), suggesting the subplasmalemmal occurrence of fast TRPV1 recycling.

Strong stimulation has been found to trap TRPV1 channels in intracellular endosomal and lysosomal networks (19). We observed a delayed recycling of TRPV1 upon high-dose capsaicin stimulation, which possibly involves the traveling through cytosolic compartments. Among Syt proteins, Syt7 orchestrates the trafficking and fusion of endosomal and lysosomal compartments (26, 27). We found that though not directly interacting

with TRPV1 (Fig. 5E), Syt7 expression inhibited the recovery of whole-cell TRPV1 current during high capsaicin-induced tachyphylaxis (Fig. 5 F and G, *light red* vs. *gray triangle*). This effect was abolished by inactivating the  $\text{Ca}^{2+}$ -binding site [Syt7 (4D/N)] (Fig. 5G), and not seen with the  $\text{Ca}^{2+}$ -insensitive Syt4 (28) (Fig. 5E and *SI Appendix, Fig. S6 C and D*). In contrast, Syt7 showed a marginal effect on the desensitization responses evoked by low-dose capsaicin (Fig. 5G). Light-sheet imaging showed that Syt7 selectively inhibited TRPV1 recycling upon high (10  $\mu\text{M}$ ), but not low (1  $\mu\text{M}$ ) capsaicin stimulation (Fig. 5H vs. Fig. 5D). Given the role of Syt7 in endosomal and lysosomal trafficking, our results likely reflect that Syt7 via enhancing interorganelle fusion hindered the targeted redelivery of TRPV1 to the plasma membrane. Also distinct from Syt1, Syt7 was expressed throughout cell cytoplasm, compatible with its role in intracellular trafficking (*SI Appendix, Fig. S7*). Together, these results suggest that Syt7 regulates slow TRPV1 recycling during high capsaicin-induced tachyphylaxis.

### Discussion

Tachyphylaxis is therapeutically relevant for pain treatment, in conditions barely tractable by conventional analgesics (3, 29). We show here that stimulation strength shapes the extent of whole-cell tachyphylaxis, as modulated by TRPV1 recycling (*SI Appendix, Fig. S8*). The observation that a persistent reduction in TRPV1 responses requires high-intensity stimuli provides a mechanistic basis for the need of large-dose capsaicin in tackling neuropathic pains (29). Exocytic insertion of TRPV1 has been suggested to tune channel expression levels in a  $\text{Ca}^{2+}$ - and SNARE-dependent manner (1, 11, 13, 18, 30–32). Relatively,

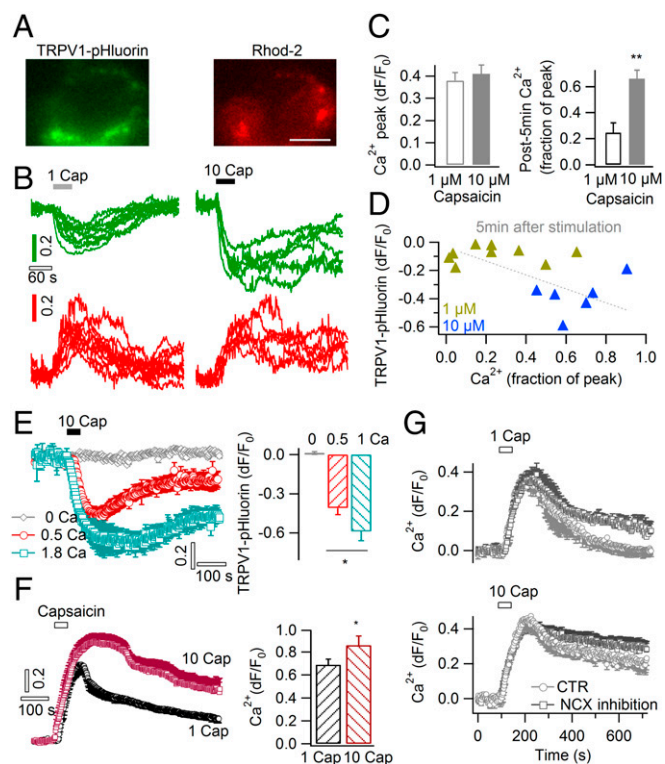


**Fig. 4.**  $\text{Ca}^{2+}$  signals during stimulation strength-gated TRPV1 recycling. (A) Representative images of HEK 293 cells expressing TRPV1-pHluorin and loaded with the red  $\text{Ca}^{2+}$  dye Rhod-2, AM. (B) Fluorescence time courses of TRPV1-pHluorin and Rhod-2 in response to 1  $\mu\text{M}$  and 10  $\mu\text{M}$  capsaicin, respectively. A single trace denotes an individual cell, and fluorescence change is expressed as  $\text{dF}/\text{F}_0$ . (C) Peak amplitude of  $\text{Ca}^{2+}$  signals and the  $\text{Ca}^{2+}$  levels at 5 min after the stimulation onset ( $n = 9$  for 1  $\mu\text{M}$ , 6 for 10  $\mu\text{M}$  capsaicin). (D) Scatter plot showing the apparent loss in TRPV1 surface expression against the corresponding  $\text{Ca}^{2+}$  levels, both measured at 5 min post the stimulation. (E) TRPV1-pHluorin recycling triggered by 10  $\mu\text{M}$  capsaicin in different concentrations of  $\text{Ca}^{2+}$  ( $n = 6-8$  cells for each condition). (F)  $\text{Ca}^{2+}$  signals evoked by 1  $\mu\text{M}$  and 10  $\mu\text{M}$  capsaicin in cells with ER  $\text{Ca}^{2+}$  ATPase inhibited by thapsigargin (0.5  $\mu\text{M}$ , pretreatment 10 min,  $n = 8$  cells for each condition). (G) Differential alteration in the declining phase of low and high capsaicin-evoked  $\text{Ca}^{2+}$  signals upon NCX inhibition ( $n = 6-10$  cells for each condition). (Scale bar, 10  $\mu\text{m}$ .)

little is known on TRPV1 endocytic retrieval, though steady-state examination a few minutes apart showed intracellular TRPV1 accumulation over capsaicin stimulation (19). Also, previous results were mostly obtained from antibody-based assays in fixed cells or extracted tissues. By light-sheet microscopy and TRPV1-pHluorin, we achieved real-time imaging of TRPV1 recycling at layers away from the cell-coverslip adhesion site. This helps to avoid potential interference of certain adhesive substrates (e.g., polylysine) to TRPV1 activity (12).

We revealed a tunable coupling between TRPV1 endocytosis and exocytosis over strength-memorizing tachyphylaxis. The time scale of TRPV1 endocytosis is comparable to that found for clathrin-mediated endocytosis, in the order of tens to one hundred seconds (33). Activity-gated recycling imposes a net effect on TRPV1 surface expression, whereby whole-cell responses over tachyphylaxis. Recent study by total internal reflection fluorescence microscopy reveals that mobile TRPV1 in the plasma membrane becomes abruptly static upon activation (34), implying a preceding step to confine TRPV1 on endocytic sites for intracellular translocation. Fluorescence resonance energy transfer unveiled TRPV1 in subplasmalemmal caveolar structures (35), suggesting their implication in channel endocytosis.

The present TRPV1-pHluorin labeling does not appear as an idea ring on the cell surface, likely because the light sheet has a thickness in the order of several microns and still collects certain amount of out-of-focus fluorescence. Also, pHluorin could be weakly fluorescent in organelles with moderate acidic levels (e.g.,

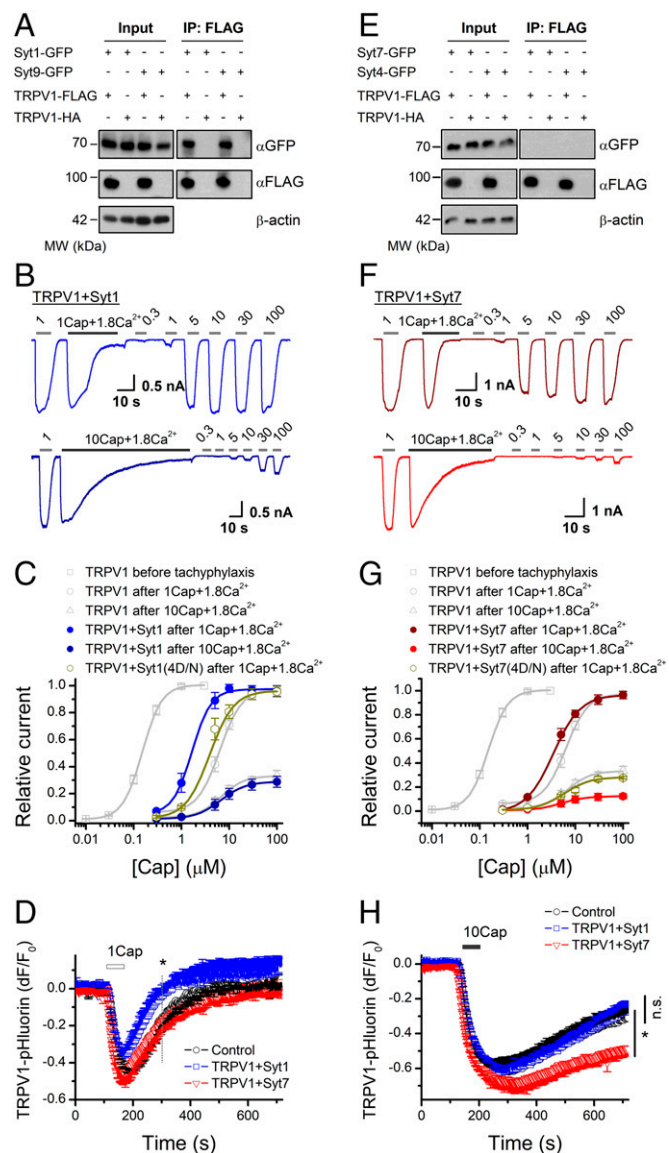


**Fig. 5.** Synaptotagmin regulation of TRPV1 recycling. (A) Interaction of Syt1 and Syt9 with TRPV1. Immunoprecipitation (IP, with anti-FLAG) and immunoblot analysis (with anti-GFP) of HEK 293 cells transfected with plasmids as indicated. Molecular weight standards (MW, in kDa) are shown on the left. (B) Whole-cell currents in HEK cells coexpressing TRPV1 and Syt1 in response to 1  $\mu\text{M}$  and 10  $\mu\text{M}$  capsaicin, respectively. (C) Pooled dose-response curves showing Syt1 facilitation of current recovery during 1  $\mu\text{M}$  capsaicin-induced tachyphylaxis (blue vs. gray open circle,  $n = 6-7$  cells for each condition; solid lines are fitting by Hill equation). Gray traces are without Syt1. (D) Low capsaicin-evoked TRPV1 recycling was facilitated by Syt1, but not by Syt7 ( $n = 8-10$  cells for each condition). TRPV1-pHluorin and red fluorescent Syt1-tdTomato were coexpressed in HEK cells, with the absence of cross-talk verified (SI Appendix, Figs. S5 and S7). (E-G) Parallel experiments to examine the interaction of TRPV1 with Syt7 and Syt4, and record their impact on whole-cell TRPV1 currents ( $n = 6-8$  cells for the pooled dose-response curves). (H) Light-sheet imaging of TRPV1 recycling upon 10  $\mu\text{M}$  capsaicin stimulation, which was retarded by Syt7 expression (Syt7-tdTomato;  $n = 9-12$  cells for each condition).

~6.3 in endosomes) (36, 37), thereby adding background signals to TRPV1-pHluorin imaging. We detected barely the recovery in TRPV1-pHluorin fluorescence upon high capsaicin stimulation in DRG neurons. It is possible that transfection of TRPV1-pHluorin in neurons may not fully substitute endogenous TRPV1 channels. Their interaction with regulatory proteins for subcellular trafficking (e.g., SNAREs and synaptotagmins) might also be tighter than TRPV1-pHluorin, which to some extent compromises the recycling rate of TRPV1-pHluorin.

Distinct  $\text{Ca}^{2+}$  signals were found during tachyphylaxis induction and TRPV1 recycling. High-dose capsaicin triggered relatively greater  $\text{Ca}^{2+}$  influx, reminiscent of TRPV1 pore dilation that is suggested to augment channel conductance and alter ion selectivity upon strong stimulation (38) (but see ref. 39). The effect of high-dose capsaicin on NCX  $\text{Ca}^{2+}$  export could be due to the possible disturbance of capsaicin, as a lipophilic molecule (2), to the local lipid environment of NCX, a factor known to alter its activity (40). In relaying  $\text{Ca}^{2+}$  signals to subcellular trafficking, members of Syt protein family behave as  $\text{Ca}^{2+}$  sensors (24). We show intriguingly that Syt1 and Syt7 regulate the fast and slow TRPV1 recycling, respectively, in a condition-specific manner. Thus, different trafficking routes are recruited by stimuli of varied strengths to regulate whole-cell TRPV1 tachyphylaxis (SI Appendix, Fig. S8). This finding also

suggests the influence of  $\text{Ca}^{2+}$  on TRPV1 trafficking going beyond the subplasmalemmal zone.

## Materials and Methods

The wild-type rat TRPV1 cDNA was generously provided by Dr. Feng Qin (State University of New York at Buffalo). TRPV1-615-pHluorin GFP (Insertion of pHluorin GFP gene after No. 614 residue of TRPV1) was made using the overlap-extension PCR method as previously described (41). Patch-clamp recordings were made in whole-cell configuration using an EPC10 amplifier (HEKA). Light-sheet imaging was performed using a wide-field upright microscope (Zeiss Axioskop 50) and an independent optical module (Alpha3 light sheet add-on, Zeiss EC EPIPlan  $\times 10$ , 0.25NA) (SI Appendix, Fig. S2A). Detailed methods are provided in SI Appendix.

**ACKNOWLEDGMENTS.** We thank Steve Didiene for fabricating imaging accessories, and Dr. Luna Gao, Mr. Yifu Han, and our colleagues for comments and discussions. We also sincerely thank Dr. Sheela Vyas for her critical reading of the manuscript. This work was supported by the National Natural Science Foundation of China (Grants 31628005, 31830031, 31671209, 31871174, 31601864, and 31728014), National Basic Research Program of China (Grant 2014CB910304), Natural Science Foundation of Hubei Province (Grants 2017CFA063 and 2018CFA016), Fundamental Research Funds for the Central Universities (Grants 2042017KF0242 and 2042017KF0199), and CAS Key Laboratory of Receptor Research (Grant SIMM1804YKF-02). The work was also supported in part by Agence Nationale de la Recherche (Grant NUTRIPATHOS, ANR-15-CE14-0030, France).

- Planells-Cases R, Valente P, Ferrer-Montiel A, Qin F, Szallasi A (2011) Complex regulation of TRPV1 and related thermo-TRPs: Implications for therapeutic intervention. *Adv Exp Med Biol* 704:491–515.
- Morales-Lázaro SL, Simon SA, Rosenbaum T (2013) The role of endogenous molecules in modulating pain through transient receptor potential vanilloid 1 (TRPV1). *J Physiol* 591:3109–3121.
- Touska F, Marsakova L, Teisinger J, Vlachova V (2011) A “cute” desensitization of TRPV1. *Curr Pharm Biotechnol* 12:122–129.
- Vyklický L, et al. (2008) Calcium-dependent desensitization of vanilloid receptor TRPV1: A mechanism possibly involved in analgesia induced by topical application of capsaicin. *Physiol Res* 57:559–568.
- Knotkova H, Pappagallo M, Szallasi A (2008) Capsaicin (TRPV1 agonist) therapy for pain relief: Farewell or revival? *Clin J Pain* 24:142–154.
- Szocsányi J (2014) Capsaicin and sensory neurones: A historical perspective. *Prog Drug Res* 68:1–37.
- Mohapatra DP, Nau C (2005) Regulation of  $\text{Ca}^{2+}$ -dependent desensitization in the vanilloid receptor TRPV1 by calcineurin and cAMP-dependent protein kinase. *J Biol Chem* 280:13424–13432.
- Lishko PV, Procko E, Jin X, Phelps CB, Gaudet R (2007) The ankyrin repeats of TRPV1 bind multiple ligands and modulate channel sensitivity. *Neuron* 54:905–918.
- Yao J, Qin F (2009) Interaction with phosphoinositides confers adaptation onto the TRPV1 pain receptor. *PLoS Biol* 7:e46.
- Bhave G, et al. (2002) cAMP-dependent protein kinase regulates desensitization of the capsaicin receptor (VR1) by direct phosphorylation. *Neuron* 35:721–731.
- Camprubi-Robles M, Planells-Cases R, Ferrer-Montiel A (2009) Differential contribution of SNARE-dependent exocytosis to inflammatory potentiation of TRPV1 in nociceptors. *FASEB J* 23:3722–3733.
- Stein AT, Ufret-Vincenty CA, Hua L, Santana LF, Gordon SE (2006) Phosphoinositide 3-kinase binds to TRPV1 and mediates NGF-stimulated TRPV1 trafficking to the plasma membrane. *J Gen Physiol* 128:509–522.
- Devesa I, et al. (2014)  $\alpha$ CGRP is essential for algescic exocytotic mobilization of TRPV1 channels in peptidergic nociceptors. *Proc Natl Acad Sci USA* 111:18345–18350.
- Ferrandiz-Huertas C, Mathivanan S, Wolf CJ, Devesa I, Ferrer-Montiel A (2014) Trafficking of thermoTRP channels. *Membranes (Basel)* 4:525–564.
- Burrone J, Li Z, Murthy VN (2006) Studying vesicle cycling in presynaptic terminals using the genetically encoded probe synaptopHluorin. *Nat Protoc* 1:2970–2978.
- Power RM, Huisken J (2017) A guide to light-sheet fluorescence microscopy for multiscale imaging. *Nat Methods* 14:360–373.
- Heuser JE, Anderson RG (1989) Hypertonic media inhibit receptor-mediated exocytosis by blocking clathrin-coated pit formation. *J Cell Biol* 108:389–400.
- Morenilla-Palao C, Planells-Cases R, Garcia-Sanz N, Ferrer-Montiel A (2004) Regulated exocytosis contributes to protein kinase C potentiation of vanilloid receptor activity. *J Biol Chem* 279:25665–25672.
- Sanz-Salvador L, Andrés-Bordería A, Ferrer-Montiel A, Planells-Cases R (2012) Agonist- and  $\text{Ca}^{2+}$ -dependent desensitization of TRPV1 channel targets the receptor to lysosomes for degradation. *J Biol Chem* 287:19462–19471.
- Jordt SE, Tominaga M, Julius D (2000) Acid potentiation of the capsaicin receptor determined by a key extracellular site. *Proc Natl Acad Sci USA* 97:8134–8139.
- Vogel SS (2009) Channeling calcium: A shared mechanism for exocytosis-endocytosis coupling. *Sci Signal* 2:pe80.
- Brini M, Carafoli E (2009) Calcium pumps in health and disease. *Physiol Rev* 89:1341–1378.
- Blaustein MP, Lederer WJ (1999) Sodium/calcium exchange: Its physiological implications. *Physiol Rev* 79:763–854.
- Südhof TC (2002) Synaptotagmins: Why so many? *J Biol Chem* 277:7629–7632.
- Lee J, Guan Z, Akbergenova Y, Littleton JT (2013) Genetic analysis of synaptotagmin C2 domain specificity in regulating spontaneous and evoked neurotransmitter release. *J Neurosci* 33:187–200.
- Trajkovic K, Jeong H, Krainc D (2017) Mutant huntingtin is secreted via a late endosomal/lysosomal unconventional secretory pathway. *J Neurosci* 37:9000–9012.
- Volynski KE, Krishnakumar SS (2018) Synergistic control of neurotransmitter release by different members of the synaptotagmin family. *Curr Opin Neurobiol* 51:154–162.
- Dai H, et al. (2004) Structural basis for the evolutionary inactivation of  $\text{Ca}^{2+}$  binding to synaptotagmin 4. *Nat Struct Mol Biol* 11:844–849.
- Robbins WR, et al. (1998) Treatment of intractable pain with topical large-dose capsaicin: Preliminary report. *Anesth Analg* 86:579–583.
- Chuang HH, et al. (2001) Bradykinin and nerve growth factor release the capsaicin receptor from PtdIns(4,5)P<sub>2</sub>-mediated inhibition. *Nature* 411:957–962.
- Zhang X, Huang J, McNaughton PA (2005) NGF rapidly increases membrane expression of TRPV1 heat-gated ion channels. *EMBO J* 24:4211–4223.
- Meng J, Wang J, Steinhoff M, Dolly JO (2016) TNF $\alpha$  induces co-trafficking of TRPV1/TRPA1 in VAMP1-containing vesicles to the plasmalemma via Munc18-1/syntaxin1/SNAP-25 mediated fusion. *Sci Rep* 6:21226.
- He K, et al. (2017) Dynamics of phosphoinositide conversion in clathrin-mediated endocytic traffic. *Nature* 552:410–414.
- Senning EN, Gordon SE (2015) Activity and  $\text{Ca}^{2+}$  regulate the mobility of TRPV1 channels in the plasma membrane of sensory neurons. *eLife* 4:e03819.
- Storti B, Di Rienzo C, Cardarelli F, Bizzarri R, Beltram F (2015) Unveiling TRPV1 spatio-temporal organization in live cell membranes. *PLoS One* 10:e0116900.
- Sankaranarayanan S, De Angelis D, Rothman JE, Ryan TA (2000) The use of pHluorins for optical measurements of presynaptic activity. *Biophys J* 79:2199–2208.
- Casey JR, Grinstein S, Orlowski J (2010) Sensors and regulators of intracellular pH. *Nat Rev Mol Cell Biol* 11:50–61.
- Chung MK, Güler AD, Caterina MJ (2008) TRPV1 shows dynamic ionic selectivity during agonist stimulation. *Nat Neurosci* 11:555–564.
- Li M, Toombes GE, Silberberg SD, Swartz KJ (2015) Physical basis of apparent pore dilation of ATP-activated P2X receptor channels. *Nat Neurosci* 18:1577–1583.
- Philipson KD, Ward R (1985) Effects of fatty acids on  $\text{Na}^{+}$ - $\text{Ca}^{2+}$  exchange and  $\text{Ca}^{2+}$  permeability of cardiac sarcolemmal vesicles. *J Biol Chem* 260:9666–9671.
- Yao J, Liu B, Qin F (2011) Modular thermal sensors in temperature-gated transient receptor potential (TRP) channels. *Proc Natl Acad Sci USA* 108:11109–11114.
- Samways DS, Egan TM (2011) Calcium-dependent decrease in the single-channel conductance of TRPV1. *Pflugers Arch* 462:681–691.